# ALN WIDEBAND ENERGY HARVESTERS WITH WAFER-LEVEL VACUUM PACKAGING UTILIZING THREE-WAFER BONDING

*Nan Wang[1], Chengliang Sun[1], Li Yan Siow[1], Hongmiao Ji[1], Peter Chang[1], Qingxin Zhang[1], and Yuandong Gu[1]*

[1]Institute of Microelectronics, A*STAR (Agency for Science, Technology and Research), Singapore

## ABSTRACT

This paper experimentally demonstrates an aluminum nitride (AlN) based piezoelectric MEMS energy harvester (EH) with an operation bandwidth of 64.6Hz (859.9Hz – 924.5Hz, 7.24%), peak output open-circuit voltage of 4.43V, and an output power of 82.24μW that yields a high power density of 0.734mW/cm$^3$ with its size of 0.8×0.8×0.175cm$^3$. The in-house microfabricated wideband EH is packaged using a novel wafer-level vacuum packaging scheme which employs two times of eutectic Al-Ge bonding to bond the device wafer to both the top cap wafer and the bottom cap wafer. In addition, Ti is employed as the getter material to enhance the vacuum level inside the cavity, hence reducing the air damping experienced by the cantilevers and increasing the quality factor (Q-factor) and output voltage. The reported EH is a promising candidate in the application of Internet of Things (IoT) to for powering various wireless sensor nodes (WSN) which are located in environment with a wide range of vibration frequencies.

## INTRODUCTION

Over recent years, wireless sensors and MEMS has attracted much research attention, especially on microactuators, microsensors, as well as microsystems obtained by integrating micromechanical devices with microelectronic for various applications. Specifically, vibration-based EHs, which are capable of converting ambient vibrational energy into usable electrical energy, are attracting serious research attention due to the increasing demand for self-powered WSN for IoT applications [1-2], in which many of these WSN are imbedded in the standalone structure or remote environments whereby physical connection to the outside world does not exist. State-of-the-art vibration-based EHs are facing the tradeoff between the operation bandwidth and the output power: on one hand, due to the narrow frequency bandwidth, the output power drops significantly when the input frequency deviates from the resonant frequency of the EH [3]; on the other hand, for current wideband EH, the output power is relatively low, typically in nW range [4]. As such, there is a need for EHs which can overcome the aforementioned tradeoff and harvest vibrational energy for a range of frequencies, in order to support self-powered WSN for IoT applications, in which the frequency of the ambient vibration varies and high output power is required [5].

## STRUCTURE DESIGN

Fig. 1 shows the designed wideband EH, which is of a multi-cantilever structure, with the resonant frequencies of each of the six constituting cantilevers being different from one another. The spring structures are identical for the six constituting cantilevers, whereas the proof mass is designed to be different from each other by etching holes with different dimensions to vary the mass reduction from the original proof mass. As such, the resonant frequencies of the constituting cantilevers are designed to be different to one another, since the resonant frequency of a cantilever is a function of spring constant and mass, and the mass varies with the spring constant being kept constant. With the constituting cantilevers having various resonant frequencies, wideband EH behavior can be observed.

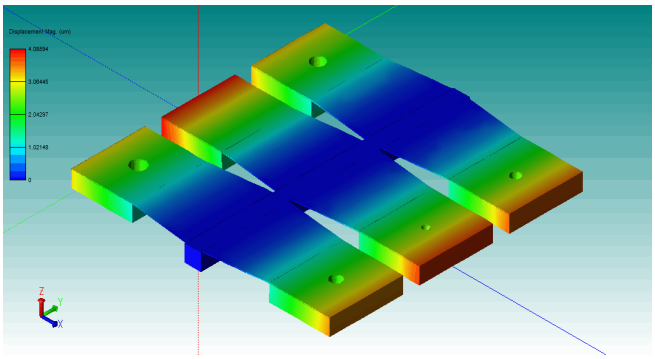

*Figure 1: 3D illustration and resonant model of the designed wideband energy harvester. By etching holes with different areas on individual cantilevers, the six cantilevers are designed to vibrate at different resonant frequencies due to the difference in the cantilevers' mass.*

The design depicted in Fig. 1 is numerically verified by commercial simulation software MEMS+™, with the simulated frequency response of the tip deflection for each of the six constituting cantilevers shown in Fig. 2 using different colors. The left most data series shown in red color corresponds to the constituting cantilever without etching hole while the right most data series corresponds to the constituting cantilever with the etching hole of the largest dimension. Since the resonant frequency of a cantilever is inversely related to the mass of the cantilever, the cantilever with the etching hole of the largest dimension has the highest resonant frequency because the effective mass remained after etching the hole is smallest. Similarly, the cantilever without any etching holes has the lowest resonant frequency, since the effective mass is largest. Each constituting cantilever is optimized to have different resonant frequencies from one another, with the frequency difference between two adjacent resonant peaks approximately equal, in order to achieve a smooth

broadband behavior. The data shown in Fig. 2 are deflection of the cantilevers' tips under the acceleration of 1.025g, in which tip displacement with peak value of 278.2µm is achieved. Given that the depth of the cavity in the cap wafers are 280µm, the acceleration of the simulation is set at 1.025g, in order to assure that the cantilevers do not touch the cap wafers and to accurately study the behavior of the cantilevers. For input accelerations above 1.025g, the deflection of the cantilevers will be larger than the depth of the cavity in the cap wafers (280µm), resulting in inaccurate study of the cantilever behavior.

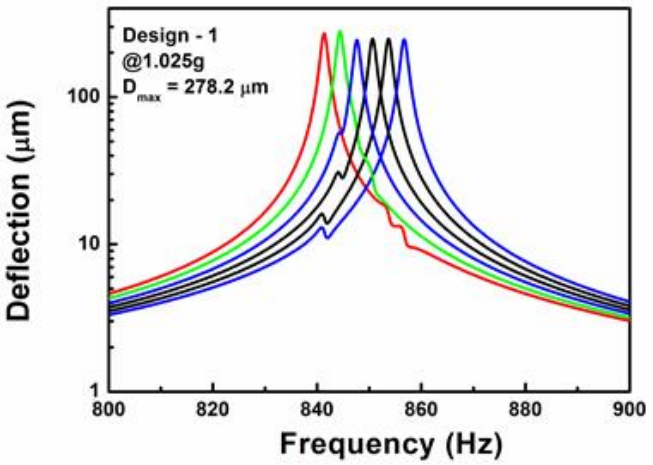


*Figure 2: Simulated frequency response of tip deflection for the six constituting cantilevers under the acceleration of 1.025g. Each constituting cantilever is optimized to have different resonant frequency from one another, with the frequency difference between two adjacent peaks approximately the same. A maximum tip displacement of 278.2µm is achieved under the acceleration of 1.025g.*

Fig. 3 shows the simulated output open-circuit voltage with input acceleration of 0.2g and 1.025g. Broadband behavior is clearly observed under both accelerations, whereas a peak open-circuit voltage of 3.43V is obtained under 1.025g. Again, such an acceleration value is chosen in the simulation study in order to study the generated open-circuit accurately by ensuring the non-contact between the tip of the cantilevers and the capping wafers, due to limited depth of the cavity in the capping wafers. Moreover, wideband behavior can also be clearly observed under low acceleration conditions of 0.2g, showing the capability of the designed wideband EH harvesting ambient vibration energy with low acceleration and varied frequency, making it suitable for WSN in IoT applications.

## FABRICATION PROCESS

From the cross-section SEM image shown in Fig. 4, each constituting cantilever is a 20µm-thick silicon beam with 1.32µm-thick AlN deposited on top and a 400µm-thick Si proof mass attached to the tip. It is then wafer-level vacuum packaged by a two-step three-wafer Al-Ge bonding: top cap wafer bonding to the device wafer followed by bottom cap wafer bonding. Cavities are etched on both cap wafers to make room for cantilevers' vibration. Ti is employed as the getter material to enhance the vacuum level of the cavity, rendering larger operation bandwidth and higher output power of the microfabricated EH by further reducing the air damping experienced by the constituting cantilevers. An optical photograph of the packaged device is also shown in Fig. 4. Detailed fabrication process is explained in the text below.

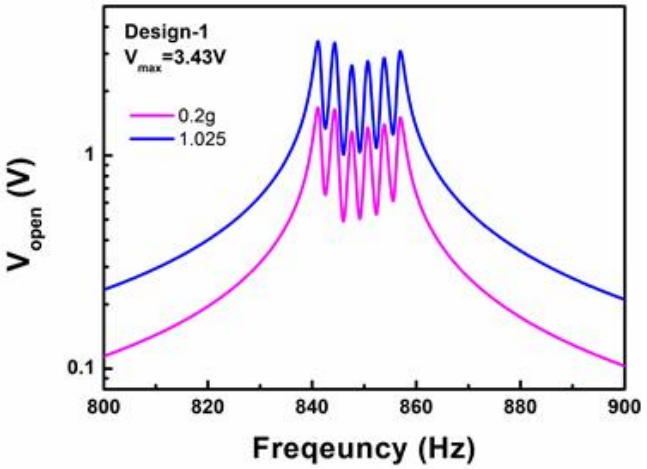


*Figure 3: Simulated output open-circuit voltage with input acceleration of 0.2g and 1.025g. Broadband behavior is observed under both accelerations, whereas a peak open-circuit voltage of 3.43V is obtained under 1.025g.*

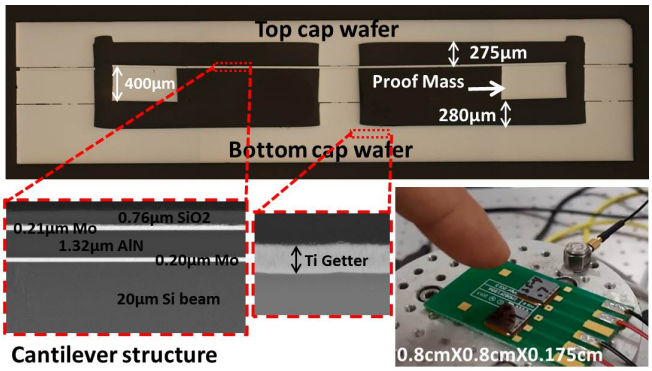


*Figure 4: Cross sectional SEM images of the integrated wideband energy harvester, which is wafer level vacuum packaged by three-wafer two-step Al-Ge eutectic bonding. Zoom-in views depicted in the insets show the thickness information of the cantilever structure and the Ti getter employed at the bottom cap wafer in order to enhance the vacuum level inside the vacuum cavity. An optical photograph is also shown on the bottom right corner with the size of the integrated wideband energy harvester chip labelled.*

For the MEMS device wafer, the fabrication starts with depositing 0.02µm AlN (seed layer) / 0.2µm Mo /1.2µm AlN / 0.2µm Mo and 0.2µm high density plasma (HDP) $SiO_2$. Wafer backside alignment is defined before top

electrode (Mo) patterning. In order to create a flat wafer surface which is critical for Al/Ge bonding, 2µm low stress $SiO_2$ is deposited and followed by chemical mechanical polishing (CMP). Subsequently, top and bottom electrode is etched and 0.7µm Al is deposited and patterned to form Al bonding seal ring and electrode pad. Finally, top release etch is defined.

For the top cap wafer, Ge and $SiO_2$ are deposited on a blanket wafer before wafer is thinned down to 550µm. Then, the deposited $SiO_2$, Ge and Si with the thickness of 2.4µm is etched, followed by Si deep reactive ion etching (DRIE) to create the cavity to contain the released device structure. MEMS device and top cap wafer is then bonded using AlGe eutectic bonding.

The first few steps of bottom cap wafer fabrication process flow are very similar to that of top cap fabrication process flow. Additionally, Ti getter is deposited using shadow mask and subsequently, the bottom cap wafer is vacuum bonded to the previously bonded top cap wafer and MEMS device wafer, creating a vacuum cavity for the cantilevers to vibrate with significantly reduced air damping.

## RESULTS AND DISCUSSIONS

The wafer-level vacuum packaged wideband EH is characterized using a standard B&K vibration testing system which comprises an electromagnetic shaker, an accelerometer, a USB controller and a power amplifier. With the fabricated wideband EH under test, together with the reference accelerometer which provides real-time acceleration data to the feedback controlling system, attached to the shaker, frequency response of the fabricated wideband EH under various accelerations can be obtained by sweeping the input frequency of the shaker.

Fig.5 depicts the frequency response of the open-circuit voltage generated by the fabricated wideband EH, under the low acceleration of 0.5g. At such low acceleration, the frequency response of the open-circuit voltage generated essentially shows the measured voltage sensitivity. A peak open-circuit voltage of 1.497V is obtained under the acceleration of 0.5g, yielding a voltage sensitivity of 2.994V/g. Furthermore, a broadband behavior can be clearly observed under this acceleration.

The measured frequency response on open-circuit output voltage of the microfabricated broadband EH under different accelerations are shown in Fig. 6, with peak value achieved to be 4.43V under the acceleration of 2.0g. Broadband behavior can be clearly observed, which is in excellent agreement with the numerically simulated value. Here, we define the bandwidth to be the frequency range in which the open-circuit output voltage obtained is greater than 0.5V. It can be observed that as the input acceleration increases from 0.2g to 1.5g, both the open-circuit output voltage and the bandwidth of the fabricated EH increases. However, as the input acceleration increases from 1.5g to 2.0g, only the bandwidth increases whereas the open-circuit output voltage experiences a small amount of increment. This is because from 0.2g to 1.5g, the increase in the amplitude of the vibration of the cantilevers leads to the increase in the output voltage, together with the bandwidth. However, from the input acceleration of 1.5g onwards, the amplitude of vibration of the cantilevers exceeds the depth of the cavity of the capping wafers and results in the contact between the cantilevers and the capping wafers, further broadening the frequency band. Since the amplitude of the vibration is limited by the depth of the cavity, the output voltage experiences a small amount of increment. Under the acceleration of 2.0g, the band width of the characterized broadband EH, in which the open-circuit output voltage obtained is greater than 0.5V, is 64.6Hz (859.9Hz – 924.5Hz), which corresponds to a width-to-center ratio of 7.24%.

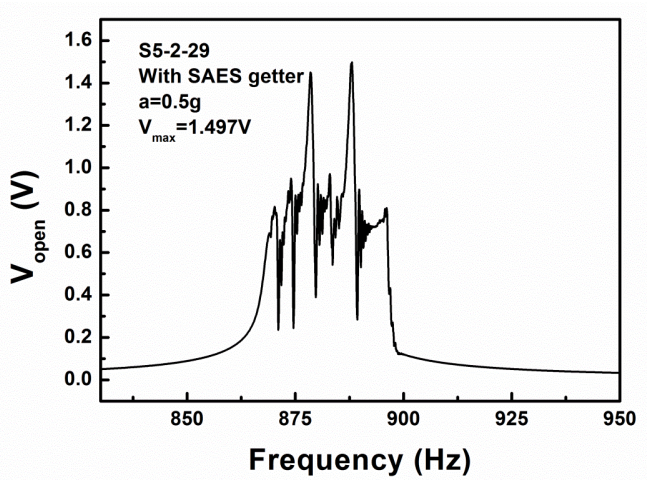


*Figure 5: Measured voltage sensitivity frequency response. A peak open-circuit voltage of 1.497V is obtained under the acceleration of 0.5g. Broadband behavior is observed.*

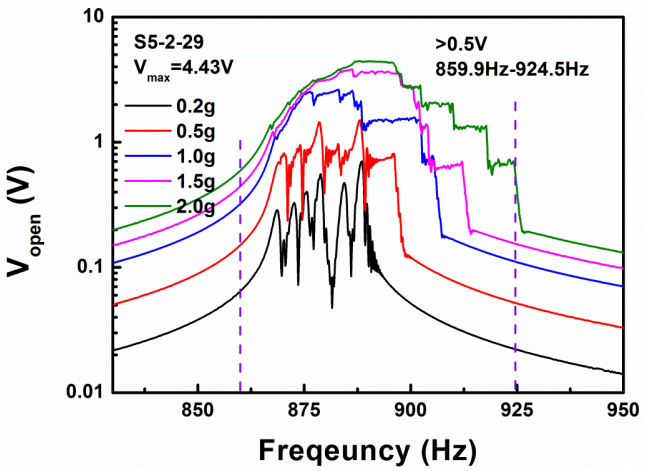


*Figure 6: Measured output open-circuit voltage of the vacuum-packaged broadband energy harvester under various accelerations. A band width of 64.6Hz (859.9Hz – 924.5Hz) is obtained, corresponding to a width-to-center ratio of 7.24%. The obtained peak open-circuit voltage is 4.43V under the acceleration of 2.0g.*

In order to measure the closed-circuit output power

spectrum of the microfabricated broadband EH, a resistor with the resistance value of 100kΩ is connected in series with the EH under test to close the circuit. The power dissipated on the resistor is then taken as the output power of the fabricated broadband EH. The measured closed-circuit output power of the broadband EH under different accelerations as depicted in Fig. 7 exhibits the same trend of the open-circuit output voltage as shown in Fig. 6, i.e., as the input acceleration increases from 0.5g to 1.5g, both the closed-circuit output power and the bandwidth of the fabricated EH increases, However, upon further increment of the input acceleration from 1.5g to 2.0g, only the bandwidth increases whereas the closed-circuit output power experiences a small amount of increment. The factors which explain this trend are very similar to those explaining the trend in open-circuit output voltage. Under the acceleration of 2.0g, the maximum closed-circuit output power achieved is 82.24μW, rendering a power density of 0.734mW/cm3 with its size of 0.8×0.8×0.175cm$^3$.

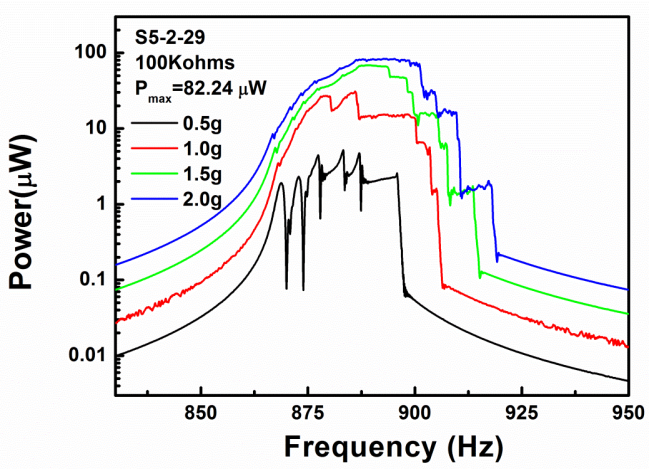


*Figure 7: Measured output power spectrum of the vacuum-packaged broadband energy harvester under various accelerations. The obtained closed-circuit peak output power is 82.24μW under the acceleration of 2.0g.*

## CONCLUSIONS

In conclusion, an AlN based piezoelectric MEMS broadband EH is designed, fabricated and experimentally characterized. The broadband EH consists of six cantilevers, whose resonant frequencies are designed to be different from one another by etching holes with various dimension on the proof mass attached to them, in order to achieve the broadband behavior. The designed broadband EH is microfabricated with the in-house AlN platform, and packaged using a novel wafer-level vacuum packaging scheme which employs two times of eutectic Al-Ge bonding to bond the device wafer to both the top cap wafer and the bottom cap wafer. In addition, Ti is employed as the getter material to enhance the vacuum level inside the cavity, hence reducing the air damping experienced by the cantilevers and increasing the quality factor (Q-factor) and output voltage. Experimental results show that an operation bandwidth of 64.6Hz (859.9Hz – 924.5Hz) which corresponds to a width-to-center ration of 7.24%, peak output open-circuit voltage of 4.43V, and an output power of 82.24μW that yields a high power density of 0.734mW/cm$^3$ with its size of 0.8×0.8×0.175cm$^3$, is obtained, making the reported broadband EH a promising candidate in IoT applications for powering various WSN in environment with a wide range of vibration frequencies.

## ACKNOWLEDGEMENTS

This work was funded by Mubadala Development Company (Abu Dhabi), Economic Development Board (Singapore) and GLOBALFOUNDRIES Singapore under the framework of 'Twinlab' project with participation of A*STAR Institute of Microelectronics (Singapore), Masdar Institute of Science and Technology (Abu Dhabi) and GLOBALFOUNDRIES- Singapore.

## REFERENCES

[1] C. B. Williams and R. B. Yates, "Analysis of a micro-electric generator for microsystems", *Sens. Actuators A, Phys.*, vol. 52, no. 1–3, pp. 8–11, Mar./Apr. 1996.

[2] S. Roundy, P.K. Wright, and J. Rabaey, "A study of low level vibrations as a power source for wireless sensor nodes", *Comput. Commun.*, vol. 26, no. 11, pp. 1131–1144, Jul. 2003.

[3] C. Sun, X. Mu, L. Y. Siow, W. M. Tsang, H. Ji, H. Chang, Q. Zhang, Y. Gu, and D.-L. Kwong, "A Miniaturization Strategy for Harvesting Vibration Energy Utilizing Helmholtz Resonance and Vortex Shedding Effect", *IEEE Electron Device Lett.*, vol. 35, no. 2, pp. 271 – 273, Feb. 2014.

[4] H. Liu, C. J. Tay, C. Quan, T. Kobayashi, and C. Lee, "Piezoelectric MEMS Energy Harvester for Low-Frequency Vibrations with Wideband Operation Range and Steadily Increased Output Power", *IEEE J. Microelectromech. Syst.*, vol. 20, no. 5, pp. 1131 – 1142, Oct. 2011.

[5] L. Bu, X. Wu, X. Wang, L. Liu *et.al.*, "Non-resonant electrostatic energy harvester for wideband applications", *Micro & Nano Lett.*, vol. 8, no. 3, pp. 135-137, Mar 2013.

## CONTACT

*Chengliang Sun, tel: +65-67705424; sunc@ime.a-star.edu.sg